Large Eddy Simulation of Fluidic Injection into a Supersonic Convergent-Divergent Duct

B. Semlitsch, M. Mihăescu, and L. Fuchs

1 Introduction

Convergent-divergent (C-D) ducts operating in supersonic flow-regimes provoke choked flow conditions in the region of the narrowest cross-section. The developed internal shocks can be unwanted for various reasons, e.g. the associate pressure losses [1]. Fluidic injection onto the exhaust of a gas turbine engine or internal fluidic injection in ducts or nozzles have been performed for various reasons, e.g. improvement of mixing, noise reduction, performance improvement, cooling, or thrust vectoring. The effect of injection was observed to depend highly on the location of injection, injection pressure, duct pressure, and inclination angle [2].

The present study investigates the behaviour of the shock-pattern inside a C-D duct, without and with fluidics. The effect of circumferential injection into the divergent part of the C-D duct is analysed. The main focus is on the transformability and the control of the shock-pattern in the duct and the disruption of the quasi-static shock-structure, with the purpose of decreasing the occurring losses in the duct.

2 Case Setup

Injection into the C-D duct is performed by using twelve cylindrical tubes of diameter D_i, equidistant spaced on the circumference of the duct. The geometry can be seen in Fig. 1. The injectors are assumed to be feed by a compressed airstream. The total temperature at the injector inlet $T_{0,i}$ was chosen to be the ambient temperature T_∞. Different tubing systems could potentially be used, but for simplicity reasons a short injection-tube is considered. The injected flow is imposed in the di-

B. Semlitsch · M. Mihăescu · L. Fuchs
Linné Flow Center and KTH Mechanics, Osquars Backe 18, 10044 Stockholm, Sweden, e-mail: {bernhard,mihai,lf}@mech.kth.se

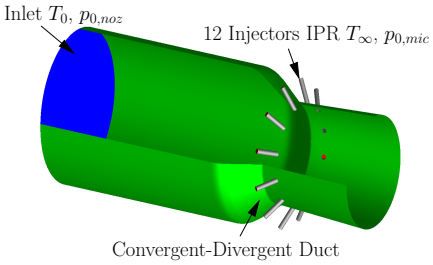

parameter	symbol	value	unit
duct exit diameter	D_e	57.5	mm
injectors diameter	D_i	2.67	mm
area ratio	$A_e/A^\star$	1.23	(-)
duct design Mach-number	$\overline{M_e}$	1.56	(-)
ambient pressure	p_∞	101,325	Pa
ambient temperature	T_∞	288.15	K

Fig. 1 The investigated geometry and the initial parameters. The injectors are located -0.857 duct exit diameters (D_e) upstream from the duct exit, i.e. in the divergent part of the duct. The tubes are inclined 60° to the duct mid-axis, and the tubes are orientated into flow direction.

rection of the injector-tubes axis, towards the centerline of the C-D duct. The tube is pressurised to a certain injection pressure ratio (IPR), defined as the injection total pressure divided by the ambient pressure.

The C-D duct is driven by a total pressure source acting at the inlet, which is four times larger than the ambient pressure p_∞ outside of the duct. At the duct inlet, the flow is assumed only in the axial direction and the total temperature $T_{0,n}$ is imposed at 367 K. The flowing media is air, where the isentropic exponent was assumed to be 1.4. Viscosity was modelled to be temperature dependent according to Sutherland's formula, where the standard coefficients where used.

3 Description of the Numerical Method

The simulations were performed with a finite volume code, solving the three-dimensional compressible Navier-Stokes equations. For the time integration, a four-stage Runge-Kutta scheme was applied. For the spatial discretisation a central difference scheme was used. A blend of second and fourth order differences are chosen to provide artificial dissipation to avoiding separation of solutions and numerical oscillations near sharp discontinuities like shocks.

Turbulence was handled by the Large Eddy Simulation (LES) approach. The turbulent small-grid scales were not modelled by any sub-grid scale (SGS) model in explicit form. The numerical dissipation acted implicitly as a SGS model.

The computational domain contains an inlet region, the investigation section, and the outer jet development region. The mesh is stretched by a factor of 1.06 to smooth out waves traveling against the flow direction. The inlet boundary is treated via a characteristic total pressure condition, where the flow is directed in the axial direction. The investigation section was designed as a fine equally cell-spaced section. The entire inner duct region (including injectors), incorporates a boundary-layer refined mesh, since the walls were treated as adiabatic, no-slip surfaces. The wall region resulted in being very important to the flow solution. Hence, a solu-

tion without modelling of the compressible boundary-layer via wall-functions was preferred.

The further jet development after the duct exit is essentially a buffer layer for modelling outlet conditions at the duct exit plane. This region stretches fifteen duct exit diameters downstream, three duct exit diameters upstream, and five duct exit diameters to the side, measured from the duct exit. The mesh is designed in such a manner that the growth factors do not exceed a value of 1.06.

4 Results & Discussions

The investigated interval of injection pressure ratios is between 1 to 5.6. The losses in the duct section are assessed by exerting the thrust equation over the duct. The thrust was monitored within the simulations and is quantified in Fig. 2. The generated thrust can be increased by a few percent using fluidic injection.

Neither the thrust nor the variation of the thrust follow a straightforward pattern. However, the change of thrust or a change in thrust variance is an indication that the flow and shock structure are significantly changed in this range of IPRs. Hence, the individual flow-field needs to be analysed, to discover the reason for this behaviour.

Without injection, one general shock pattern occurs in the duct. For the IPR of 5.6, local stocks evolve in the vicinity of injection. However, only one general shock-pattern spans over the entire duct length. In the intermediate range two intersecting shock-pattern occur.

The *baseline* case, is defined as running the duct at the duct pressure ratio of 4 without injection. Hence, IPR is one. This case can be seen in Fig. 3a, where the upper half shows the instantaneous Mach-numbers, while the lower half illustrates the density gradient. Inside of the duct, nearly inviscid conditions are present due to the large Reynolds number flow. Due to the damping effects of the compressible flow and the absence of turbulence, the variance in the generated thrust is low. However,

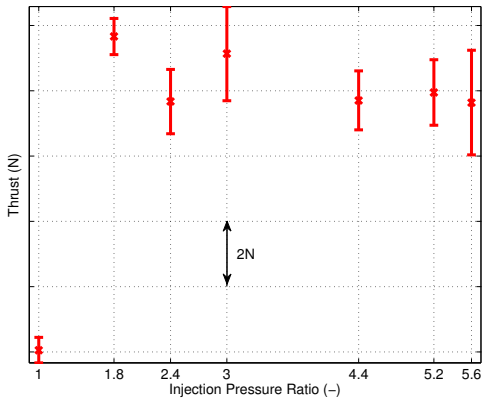

Fig. 2 The mean and the variance of the resulting thrust performance of the C-D duct is illustrated as a function of IPR. The thrust was computed including the pressure term and respecting the total demanded momentum in the injection tubes. Values were sampled at cut planes with a distance to the inlet boundaries. The fluctuations imposed by the fluidic injections lead to a variance in the generated thrust.

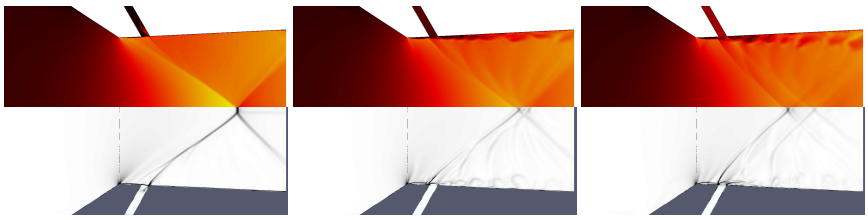

Fig. 3a IPR 1.0 **Fig. 3b** IPR 1.8 **Fig. 3c** IPR 2.4

a small separation bubble can be observed after the sharp transition passage and an expansion-fan establishes in the front of it at the smallest cross-section. Slightly downstream, at the middle of the separation bubble, a lambda shock forms one of its roots. Due to the sharp transition from the convergent section of the duct to the divergent section a shock pattern arises from this root.

The separation bubble stretches to the downstream located intersection of injection tube and the duct wall. The other lambda shock-root forms from this location, stronger than the one sitting on the separation bubble the branches of the shock-structure merge in the middle into a Mach-disk. From the Mach-disk a slip-line forms and the incident shock is reflected.

The shock-pattern occurring for the baseline case can be considered as static in the investigated section of the duct. Not any unsteady shock motion could be observed during the unsteady simulation.

By considering fluidics, at high injection pressure ratios IPR $\geq$ 2.4, the shock-pattern can be significantly altered compared to the baseline. The separation bubble occurring at the narrowest cross-section increases in its height with increasing IPR. For very low injection pressures, the injected flow creeps along the duct walls in the cross-stream, as it can be seen in Fig. 3b for an injection pressure ratio of 1.8. The vortical structures created due to injection are creeping along the nozzle walls, and do not cause turbulent fluctuations in this section. Even low injection pressure ratios cause a bow-shock in front of the injection, which replaces the lambda-shock roots observed at baseline. Several curved expansion-waves can be seen in the region between the first shock and its reflection. The shock-structure is not influenced drastically compared to the baseline case. The Mach-disk disappeared and a second weak shock-pattern becomes visible. The increase of IPR from 1.8 to 2.4 leads to a separation of the two shock-patterns (Figs. 3b and 3c). The reflection of the first shock-pattern becomes weaker and weaker with increased IPR. Also remarkable is that after a certain injection pressure ratio, the first reflected shock branch seams to disappear and does not cause any further shock-reflections.

The second downstream shock-pattern has the roots on the injected stream and the shock angles are, in the first occurring instances, almost equal with those from the first upstream located shock. With increasing injection pressure the second downstream located shock becomes stronger and the upstream located shock-pattern gets weaker. The transition of the downstream shock-pattern becoming stronger than the upstream shock-pattern, occurs between an IPR of 2.5 and 2.7.

The static pressure distribution at the duct exit is increased with injection. Hence, due to the additional injected mass, the expansion rate is lower for the jet in the divergent section. As a result of that, the first shock changes its angle and becomes almost normal with increased IPR and finally reduces to a bow-shock in front of the injection, as illustrated in Fig. 4 showing the instantaneous Mach-number (above) and density gradient (below). It was also observed that, the second shock-pattern at high injection pressure ratios is quite static, although the shock feeding expansion waves show remarkable transient motion. The second shock-pattern provokes initially a regular reflection, while a Mach-reflection starts to occur at higher injection pressure ratios.

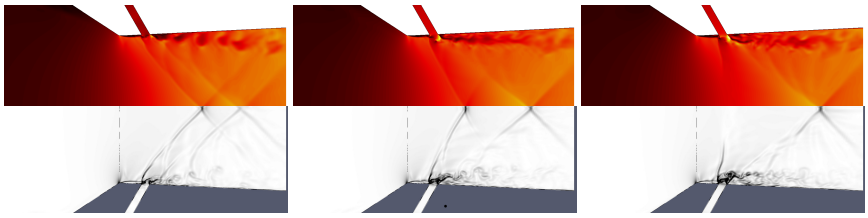

Fig. 4a IPR 3.0 **Fig. 4b** IPR 4.4 **Fig. 4c** IPR 5.6

Between an IPR of 3.0 and 4.4 the injected flow chokes as leaving the injection tubes. Once the injected flow is choked, the generated vortical structures duet injection become less coherent and their shedding frequency increases in accordance with the fact that the structures are smaller in size. Fig. 5a and Fig. 5b show a λ_2 visualisation of the flow structures occurring at an IPR of 3.0 and 4.4, respectively. The shopped like horseshoe vortices persisting undisturbed for a longer time for the not-choked case of IPR 3.0, while for an IPR of 4.4 the structures evolve more chaotic. For the case of IPR 3.0, the larger structures and the lower shedding frequency most probably cause the increased thrust variation displayed in Fig. 2.

Supporting the observation for the thrust estimations, the losses provoked due to the shocks can be illustrated by the density plots along the centreline of the duct and along an axial and an axial line at half radius, (Fig. 6a and Fig. 6b). It can be

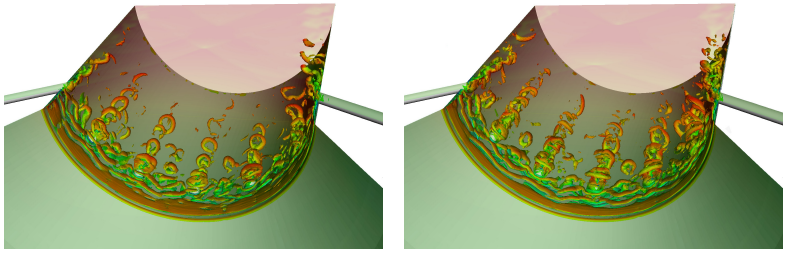

Fig. 5a λ_2 visualisation at IPR 3.0. **Fig. 5b** λ_2 visualisation at IPR 4.4.

observed that the shock strength is a minimum for the case of using injection at an IPR of 1.8.

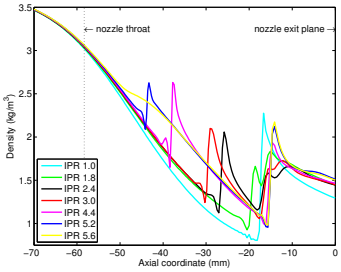

Fig. 6a Midline: Time-averaged density.

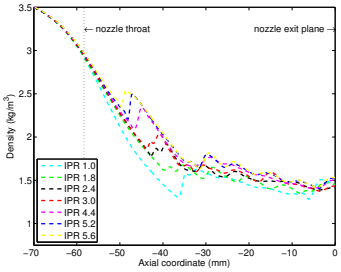

Fig. 6b Time-averaged density at half radius.

5 Conclusions

LES simulations of fluidic injection, using twelve cylindric circumferential disposed tubes, into the divergent section of a supersonic C-D duct have been performed. The improvement of performance control by transforming the occurring shock-pattern has been assessed. A range of cases have been simulated, investigating the optimisation parameter injection pressure ratio.

The reduction of losses using fluidic injection have been exhibited by the means of density gradient and thrust penalty. The thrust generation could be increased by a few percent compared to the baseline. The occurring increased variance in several cases of the thrust estimations could be explained by the generated vortical structures in the flow and the shifting of the shock-systems.

Acknowledgements This work was supported by the Swedish National Infrastructure for Computing (SNIC 002-12-11) via PDC.

References

1. Munday D., Gutmark E., Liu J. and K. Kailasanath K.: Flow structure and acoustics of supersonic jets from conical convergent-divergent nozzles. Physics of Fluids **23**, 116102 (2011).
2. Semlitsch B., Mihăescu M., Fuchs L. and Gutmark E.: Numerical Investigation of Fluidic Control on Supersonic Jet of a Gas Turbine Engine. In proceedings: 20th International Shock Interaction Symposium, pp. 161-164, (2012).